

A Zn Metal–Organic Framework with High Stability and Sorption Selectivity for CO₂

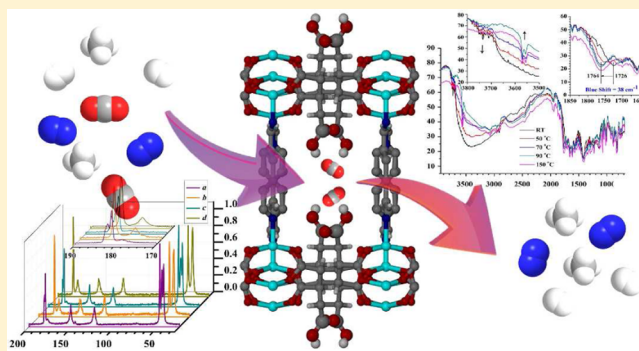
Rongming Wang,[†] Xiaobin Liu,[†] Dongdong Qi,[‡] Yuwen Xu,[†] Liangliang Zhang,[†] Xiaoqing Liu,[†] Jianzhuang Jiang,^{*‡} Fangna Dai,[†] Xin Xiao,[‡] and Daofeng Sun^{*†}

[†]State Key Laboratory of Heavy Oil Processing, College of Science, China University of Petroleum (East China), Qingdao, Shandong 266580, China

[‡]Beijing Key Laboratory for Science and Application of Functional Molecular and Crystalline Materials, Department of Chemistry, University of Science and Technology Beijing, Beijing 100083, China

S Supporting Information

ABSTRACT: A three-dimensional porous Zn metal–organic framework (UPC-12) with high thermal and chemical stability was isolated in high yield and purity from a hydrothermal reaction. UPC-12 exhibits high selectivity for CO₂ due to the formation of hydrogen bonds between CO₂ molecules and the –COOH groups exposed inside the channels and the effective π – π interactions between CO₂ molecules and the pillared bipyridine moieties of the MOF. The adsorption–desorption process was studied, for the first time, by both ¹³C CP-TOSS NMR spectroscopy and in situ DRIFTS.



INTRODUCTION

Capturing CO₂ to prevent global warming due to the greenhouse effect has been one of the most important issues in recent years.¹ Depending on the formation of C–N covalent bonds, alkanol amines have been employed to develop a quite common “amine-scrubbing” strategy/method for selective capture of CO₂ nowadays.² However, despite the effective fixation of CO₂ molecules, breaking the C–N bonds to regenerate the adsorbents unambiguously consumes quite a large amount of energy, resulting in significantly increased cost.^{2,3} On the other hand, selective separation/removal of CO₂ is also very important and indispensable for the purification of natural gas in industry since the coexisting acidic CO₂ not only significantly lowers the calorific value but also causes serious corrosion of pipelines and equipment.⁴ As a consequence, new materials possessing both high selectivity for and facile release of CO₂ are highly desired.

Because of the easy synthesis and low regeneration cost related to the usual physisorption mechanism, porous metal–organic frameworks (MOFs) that selectively adsorb CO₂ have received increasing attention in recent years in gas capture and separation.^{5,6} The utilization of open metal sites, flexible frameworks, interpenetrated frameworks, and surface-functionalized frameworks has been found to increase the selectivity and improve the separation of CO₂ from other gases.⁷ Among these, the surface functionalization method using different functional groups like –OH, –NH₂, and –SO₂ to modify the MOF pore surface seems to be the most promising one because of the effective optimization of the CO₂ selectivity and

separation ability.^{8–12} Unfortunately, most of these porous MOFs are sensitive to moisture and in particular to acidic or basic conditions. Furthermore, it is especially critical to understand the CO₂–host interactions in MOFs for the design and synthesis of porous materials with high selectivity for CO₂. As a choice, solid-state NMR spectroscopy is a powerful technique for detecting adsorbed CO₂ molecules in porous materials, as has been reported in the literature.¹³ However, detailed studies of the CO₂ adsorption–desorption process through ¹³C cross-polarization total suppression of spinning sidebands (CP-TOSS) NMR spectroscopy remain unexplored to date. Moreover, no studies of the CO₂ desorption process through in situ diffuse-reflectance infrared Fourier transform spectroscopy (DRIFTS) have been reported to date. Herein we describe the preparation, structure, and gas adsorption properties, in particular the highly selective CO₂ adsorption, of a porous –COOH surface-decorated MOF, Zn₂(H₂chhca)-(bipy)·4H₂O (UPC-12) (UPC = China University of Petroleum, H₆chhca = cyclohexane-1,2,3,4,5,6-hexacarboxylic acid, bipy = 4,4′-bipyridine), with high thermal and chemical stability. ¹³C CP-TOSS NMR and in situ DRIFTS technologies were employed to study the interactions between the adsorbed CO₂ molecules and the framework at room temperature, which are further rationalized on the basis of theoretical calculations.

Received: June 4, 2015

Published: October 27, 2015

EXPERIMENTAL SECTION

Materials and Methods. Commercially available reagents were used as received without further purification. Elemental analyses (C, H, N) were performed with a PerkinElmer 240 elemental analyzer. Thermogravimetric analysis (TGA) was performed under N₂ on a PerkinElmer TGA 7 instrument. ¹³C CP-TOSS NMR spectra were recorded on a 400 MHz Bruker Avance III spectrometer. In situ DRIFTS spectra were measured on a Nicolet Nexus infrared spectrometer.

Synthesis of UPC-12. Zn(NO₃)₂·6H₂O (223 mg), cyclohexane-1,2,3,4,5,6-hexacarboxylic acid (87 mg), and 4,4'-bipyridine (78 mg) in a molar ratio of 2:1:1 and distilled water (8 mL) were mixed in a 25 mL Teflon cup, and the mixture was shaken in an ultrasonic bath for 30 min. The vessel was then sealed and heated at 120 °C for 48 h. The autoclave was subsequently allowed to cool to room temperature. After washing with distilled water and ethanol, plate-shaped transparent colorless crystals were obtained in 90% yield. Elemental analysis of UPC-12: calcd C 37.58%, H 3.44%, N 3.98%; found C 37.20%, H 3.36%, N 3.87%.

Single-Crystal Structure Analysis. The crystallographic data and structure refinement parameters of UPC-12 are summarized in Table 1. Single-crystal X-ray diffraction of UPC-12 was performed using an

vacuum at 150 °C for 10 h to generate a solvent-free sample. A sample of 100 mg was used for gas adsorption measurements.

Theoretical Calculations. Density functional theory (DFT) calculations were carried out at the PBE-D(Grimme)/DND(3.5) level.¹⁴ The input MOF skeleton without CO₂ molecules was obtained from the single-crystal structure. The CO₂ molecules were added into the input MOF skeleton according to the possible directions of O...H hydrogen bonds in the CIF file of the single-crystal structure. Optimization of the CO₂@MOF supramolecular system was carried out at the PBE-D(Grimme)/DND(3.5) level¹⁴ in DMol³ Software¹⁵ with the global cutoff radii set to 3.0 Å.

Preparation of the CO₂-Loaded MOF for NMR Measurements. The as-synthesized sample of UPC-12 was put into zirconia rotor with a diameter of 4 mm. Subsequently, the rotor was placed in the sample tube of the micropore analyzer (ASAP 2020HD88), degassed for 10 h at 150 °C, and backfilled with CO₂. Then the rotor was taken out and capped with the lid quickly for the ¹³C CP-TOSS NMR investigation.

In Situ DRIFTS Investigation. The as-synthesized sample of UPC-12 was degassed for 5 h at 150 °C and backfilled with CO₂, and the in situ DRIFTS investigation was performed under an atmosphere of N₂ from room temperature to 150 °C and then back to room temperature. The spectra were recorded at intervals of 20 °C during heating, 40 °C during cooling from 150 to 70 °C, and 20 °C during cooling from 70 °C to room temperature. At every temperature point, two figures were scanned with a resolution of 4 cm⁻¹ and a scan time of 128 s.

Table 1. Crystal Data Collection and Structure Refinement for UPC-12

formula	C ₁₁ H ₁₂ NO ₈ Zn
<i>M_r</i>	351.58
size [mm ³]	0.17 × 0.14 × 0.11
crystal system	monoclinic
space group	<i>P2₁/n</i>
<i>a</i> [Å]	8.6256(6)
<i>b</i> [Å]	14.0418(7)
<i>c</i> [Å]	10.9059(6)
<i>α</i> [deg]	90.00
<i>β</i> [deg]	105.697(7)
<i>γ</i> [deg]	90.00
<i>V</i> [Å ³]	1271.65(13)
<i>Z</i>	4
<i>F</i> (000)	672
<i>ρ</i> _{calcd} [g cm ⁻³]	1.473
[mm ⁻¹]	7.45
range [deg]	3.49 to 25.00
reflections collected	2231
independent reflections	1722 (<i>R</i> _{int} = 0.0435)
parameters	203
<i>R</i> ₁ [<i>I</i> > 2σ(<i>I</i>)]	0.0604
<i>wR</i> ₂ [<i>I</i> > 2σ(<i>I</i>)]	0.1729
goodness of fit	1.085

Agilent Technologies SuperNova Atlas dual system with a Mo *Kα* radiation ($\lambda = 0.71073$ Å) microfocus source and focusing multilayer mirror optics. The structure was solved by direct methods using SHELXTL and refined by full-matrix least-squares on *F*² using SHELX-97. Non-hydrogen atoms were refined with anisotropic displacement parameters during the final cycles. Hydrogen atoms were placed in calculated positions with isotropic displacement parameters set to 1.2 × *U*_{eq} of the attached atom. Crystallographic data for the structures reported in this paper (excluding structure factors) have been deposited with the Cambridge Crystallographic Data Centre (CCDC 1055675).

Gas Adsorption Measurements. A freshly prepared sample (~120 mg) was soaked in CH₂Cl₂ for 24 h, and the extract was discarded. Fresh CH₂Cl₂ was subsequently added, and the sample was allowed to soak for another 24 h. This process was repeated three times to remove water solvates. Then the sample was dried under

RESULTS AND DISCUSSION

Description of the Crystal Structure. The hydrothermal reaction of cyclohexane-1,2,3,4,5,6-hexacarboxylic acid (H₆chhca), Zn(NO₃)₂, and 4,4'-bipyridine (bipy) led to the isolation of large crystals of UPC-12 in yields as high as 90%. The powder X-ray diffraction (PXRD) pattern recorded for the single-crystal sample closely matched the simulated one generated according to corresponding single-crystal diffraction results as detailed below, indicating the high purity of this target compound. Single-crystal X-ray diffraction analysis revealed that the three-dimensional (3D) porous framework of UPC-12 bears a Zn₂(COO)₄ paddlewheel secondary building unit (SBU) and that only four of the six carboxylate groups in H₆chhca (with a chair conformation) get deprotonated, resulting in the H₂chhca ligand with two protonated carboxylate groups left (Figures 1 and S1). Each of the four deprotonated carboxylate groups in H₂chhca then bridges two zinc ions, leading to the generation of a two-dimensional (2D) planar supramolecular structure along the *ac* plane with a Zn₂(COO)₄ paddlewheel SBU. This layerlike 2D planar structure, as a building block, further packs into a 3D framework with bipy ligands as pillars along the *b* axis, dependent on the coordination bonding interactions between Zn ions of the 2D supramolecular structure and nitrogen atoms of the bipy ligands, with one-dimensional (1D) channels with the dimensions of 4.15 Å × 7.23 Å (from atom to atom). In the case that H₂chhca is simplified as a 4-connected planar linker, the Zn₂(COO)₄ paddlewheel SBU as a six-connected node, and bipy as a linear linker, obviously an *psc* topology is employed by the 3D framework of UPC-12. At the end of this paragraph, it is worth noting that all of the remaining protonated carboxylate groups for all of the H₂chhca ligands in the 3D framework of UPC-12 are located inside the 1D channels (Figure 1e), rendering the channels a typical hydrophilic nature. This in turn is responsible for the selective adsorption of CO₂ by UPC-12 as detailed below.

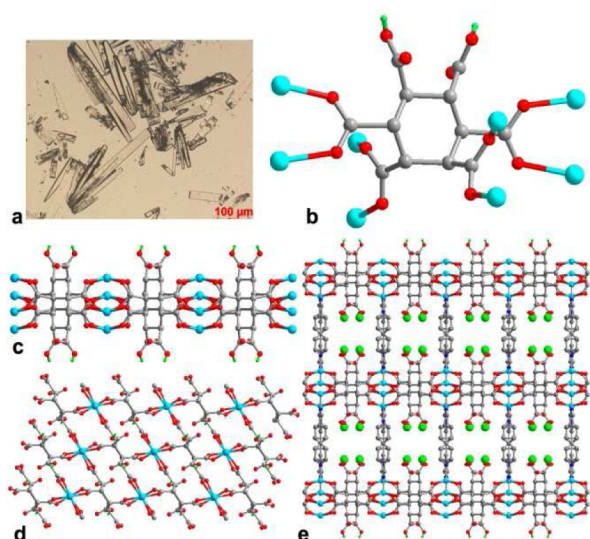


Figure 1. (a) Photograph of the UPC-12 single crystals. (b) Coordination mode of the H₂chhca ligand. (c, d) 2D layer viewed along the *c* and *b* axes, respectively. (e) 3D porous framework of UPC-12, showing the protonated carboxylate groups located inside the channels.

Thermal and Chemical Stability. TGA technology was first used to measure the stability of UPC-12 in the present case. As shown in Figure S3, the sample remains stable up to 360 °C without decomposing, indicating the high thermal stability of UPC-12. This was further confirmed by the temperature-dependent PXRD results. As clearly exhibited in Figure 2, as the temperature increases from 25 to 350 °C, the PXRD pattern remains almost unchanged in terms of both the number and positions of the peaks, indicating the unchanged framework of UPC-12 over this temperature range. This is also true for crystals of UPC-12 upon treatment in boiling water or soaking in acidic or basic aqueous solutions over the pH range of 3–12 for 24 h, revealing the high chemical stability of UPC-12. This high chemical stability may derive from the tight structure with small channels as well as the existence of protonated carboxylate groups in the framework. Despite the claimed high stabilities of several MOFs, including NO₂-tagged UiO-66, PCN-225, and pyrazole-based Ni-MOF,¹⁶ seldom have

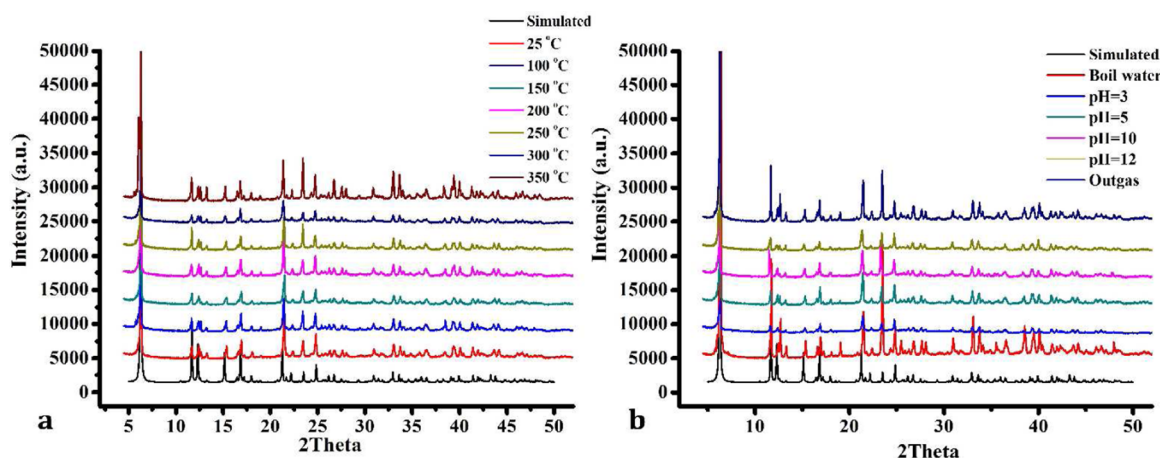


Figure 2. PXRD patterns of UPC-12: (a) patterns from room temperature to 350 °C; (b) patterns of samples with distinct chemical treatments.

porous MOFs been reported to be stable in both acidic and basic aqueous solutions.

Gas Sorption Properties. Because of the 1D channels with exposed –COOH groups involved in the framework together with its high thermal and chemical stabilities, gas uptake measurements on desolvated UPC-12 for a series of gases including N₂, CH₄, H₂, and CO₂ were carried out to study its gas adsorption properties. According to the adsorption isotherms shown in Figure 3, amounts of 6, 4.6, and 10.5

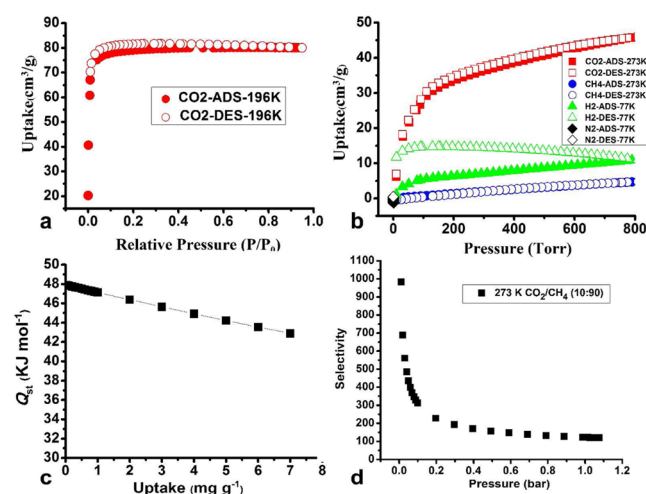


Figure 3. (a) CO₂ adsorption and desorption isotherms at 196 K. (b) Gas adsorption and desorption isotherms for CO₂ at 273 K, CH₄ at 273 K, H₂ at 77 K, and N₂ at 77 K. (c) Isothermic heat of adsorption for CO₂. (d) IAST CO₂/CH₄ selectivities for a 10:90 CO₂/CH₄ gas mixture at 273 K.

cm³ g^{−1} were deduced for adsorption of N₂ at 77 K, CH₄ at 273 K, and H₂ at 77 K, respectively, indicating the very much restricted adsorption behavior of UPC-12 for these gases. The restricted sorption behaviors for N₂, CH₄, and H₂ should result from the hydrophilic nature of the channels with a large amount of exposed protons. It should be pointed out that the anomalous behavior of the H₂ desorption isotherm is due to kinetic reasons. However, UPC-12 can selectively adsorb CO₂ molecules at 196 K with reversible type-I behavior with a Brunauer–Emmett–Teller (BET) surface area of 271.8 m² g^{−1} and a pore volume of 0.126 cm³ g^{−1}, indicating the high affinity

of the UPC-12 framework for CO₂ molecules. This was further confirmed by CO₂ adsorption measurements at different temperatures. As can be seen in Figure S4, UPC-12 exhibits typical type-I adsorption behavior for CO₂ at 273, 283, and 295 K with the adsorption abilities of 46, 38.1, and 34 cm³ g⁻¹. Furthermore, from fits of the CO₂ adsorption isotherms at 273, 283, and 295 K to a virial-type expression, a value of ~48 kJ mol⁻¹ for the isosteric heat of adsorption (Q_{st}) of UPC-12 for CO₂ at zero coverage was derived, suggesting the high selectivity of this single-crystal framework for CO₂.¹⁷ In addition, on the basis of the experimentally recorded adsorption isotherms of UPC-12 for both CO₂ and CH₄ at 273 K, ideal adsorbed solution theory (IAST) was used to further evaluate the adsorption behavior of UPC-12 for mixed gas. According to the calculation results for the 10:90 CO₂/CH₄ gas mixture (Figure 3d), in the low pressure range UPC-12 exhibits excellent selectivities for CO₂ over CH₄ ranging from 689 to 190, revealing the potential application of UPC-12 in separation of CH₄ from CO₂. Furthermore, UPC-12 also exhibits excellent selectivity for CO₂ over CH₄ at 295 K (Figure S5), which indicates that the framework of UPC-12 possesses a high affinity for CO₂ molecules.

Theoretical Investigations. DFT calculations were then performed to rationalize the high Q_{st} and selectivity of UPC-12 for CO₂ gas. The results showed that the carboxylate groups of the H₂chhca ligand located inside the channels of the framework play a very important role in the high affinity of UPC-12 for CO₂, as they form hydrogen bonds with the CO₂ molecules adsorbed at positions I, II, III, and IV with OH...O=C=O bond length of 2.48, 2.51, 2.30, and 2.48 Å, respectively (Figure 4). In combination with the π ...

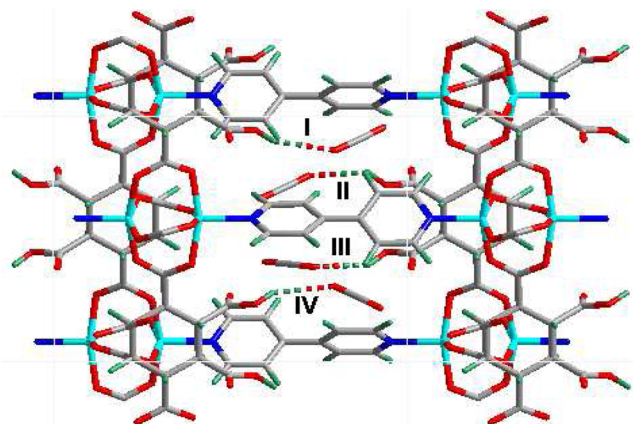


Figure 4. DFT-calculated model of the CO₂ binding sites inside the channels of UPC-12.

interactions between the π electronic structure of CO₂ (O=C=O) and the π moieties of the pillared bipy ligands in the UPC-12 framework (–C₆H₄N–) with distances in the range of 3.35–3.80 Å, this becomes responsible for the high isosteric heat of adsorption of UPC-12 for CO₂, with an average binding energy of –54.19 kJ mol⁻¹ according to the calculation results. This is in good accordance with the experimental findings as detailed above.

¹³C NMR Investigation. The high binding energy revealed for UPC-12 and CO₂ in the present case seems to suggest a quite strong combination between UPC-12 and CO₂ (actually, the stable adsorption of CO₂ gas by the MOF framework). As a consequence, solid-state ¹³C CP-TOSS NMR spectroscopy was

employed to probe the CO₂ molecules adsorbed on the UPC-12 framework at room temperature. As shown in Figure 5, four

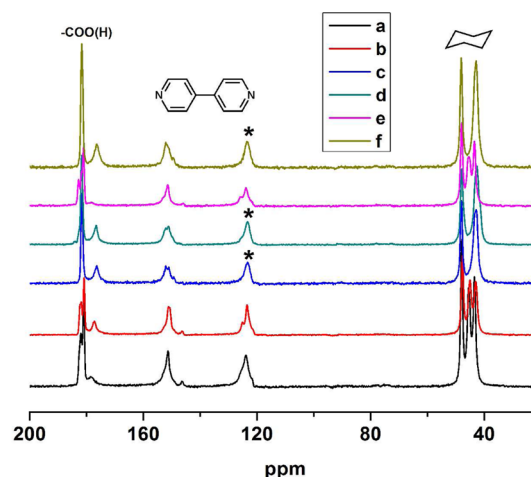


Figure 5. Solid-state ¹³C NMR spectra of UPC-12: (a) spectrum of the as-synthesized sample; (b–d) spectra after the as-synthesized sample was (b) degassed for 10 h at 150 °C, (c) degassed for 10 h at 150 °C and backfilled with CO₂, and (d) degassed for 10 h at 150 °C and allowed to stand for 2 h in air; (e) spectrum after the CO₂-loaded sample was degassed for 5 h at 150 °C and backfilled with H₂O; (f) spectrum after the H₂O-loaded sample was re-degassed for 5 h at 150 °C and re-backfilled with CO₂. Asterisks denote the CO₂ peak combined with one of the bipy peaks.

sets of signals at around 43–48, 123, 151, and 177–182 ppm due to the cyclohexane, bipy (123 and 151 ppm), and H₂chhca carboxylic carbons, respectively, were observed in the ¹³C NMR spectrum of the empty UPC-12 single-crystal sample (Figure 5b), which is similar to the spectrum of the as-synthesized sample (Figure 5a). Among the latter set of signals, the peak at 180.9 is attributed to the uncoordinated carboxyl carbons of H₂chhca in the framework, while the peaks at 177.2 and 181.8 ppm are due to the carbons of the Zn-coordinated carboxyl groups. After CO₂ was backfilled into the crystalline sample (which was first activated at 150 °C for 10 h) and kept for half an hour, significant changes in the ¹³C NMR spectrum occur (Figure 5c) as a result of the formation of hydrogen bonds between the uncoordinated carboxyl groups of H₂chhca and the CO₂ molecules adsorbed inside the channels. The peak at 180.9 ppm disappears, while along with a slight low-field shift the peak at 181.8 ppm becomes sharpened. Also, as a result of the hydrogen-bond formation by the two uncoordinated carboxyl groups left for H₂chhca, the triplet signal at 43–48 ppm due to the cyclohexane carbons becomes a doublet as a result of the concomitant environmental change. In addition, the peak at 123 ppm with almost the same intensity as the one at 151 ppm for the empty UPC-12 single-crystal sample becomes obviously stronger than that at 151 ppm after treatment of empty UPC-12 with CO₂. This result appears to suggest that the CO₂ molecules adsorbed resonate at 123 ppm,¹⁸ which overlaps with the peak of the bipy carbons at the same position to intensify the signal. Further support was provided by the following experimental results. The ¹³C CP-TOSS NMR spectrum after the empty MOF was put in the air at room temperature for 2 h (Figure 5d) is similar to that of the CO₂-loaded MOF, demonstrating that the empty MOF can adsorb CO₂ from the air. In addition, the CO₂-loaded sample was put into a tube and heated to 150 °C under vacuum for 5 h to release the adsorbed

CO₂, and the resulting MOF sample was then directly poured into water to avoid CO₂ contamination. The ¹³C NMR spectrum of this newly treated sample (Figure 5e) was found to be almost identical with the spectrum of the as-synthesized MOF. Nevertheless, the ¹³C NMR spectrum of the CO₂-adsorbed sample was completely recovered after this sample was reactivated and re-backfilled with CO₂ (Figure 5f).

In Situ DRIFTS Study. In situ DRIFTS was also utilized to confirm the stable adsorption of CO₂ gas by the UPC-12 framework. Figure 6 displays the temperature-dependent in situ

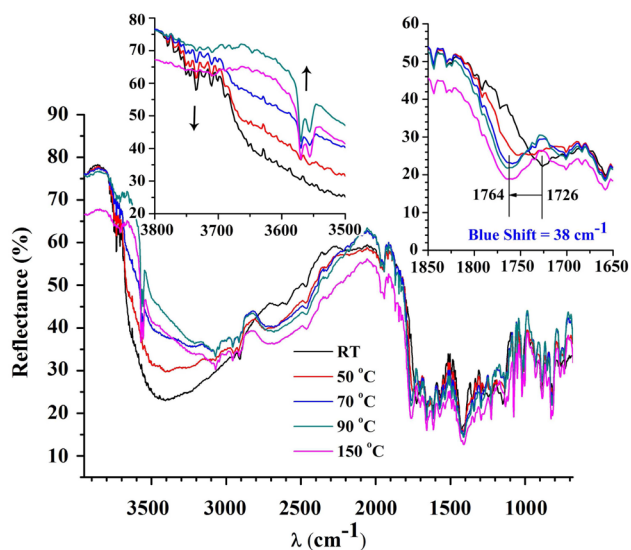


Figure 6. In situ DRIFTS spectra, recorded under a flowing N₂ atmosphere, of a CO₂-loaded sample of UPC-12 at room temperature and upon heating to 50, 70, 90, and 150 °C.

DRIFTS spectra of the CO₂-loaded sample under a flowing N₂ atmosphere. The observation of the peak at 1792 cm⁻¹ due to the asymmetric stretching vibration of CO₂ (ν_1) as well as the absorptions at 3735 and 3750 cm⁻¹ due to the combination mode arising from ν_1 and the bending mode of CO₂¹⁹ in the room temperature spectrum clearly demonstrates the existence of the CO₂ molecules adsorbed inside the channels of UPC-12. The peak at 1726 cm⁻¹ observed in this spectrum is attributed to the carbonyl stretching vibration of the -COOH groups of H₂chhca after hydrogen-bond formation with CO₂ molecules, and it is accompanied by the appearance of a broad O-H stretching vibration peak at 3406 cm⁻¹.^{8c} Along with the gradual release of the adsorbed CO₂ by heating of the sample from room temperature to 50, 70, 90, and 150 °C, the absorptions at 3735 and 3750 cm⁻¹ gradually lose intensity in the same order and ultimately disappear in the 150 °C in situ DRIFTS spectrum. Meanwhile, the carbonyl stretching vibration peak of the -COOH groups undergoes a gradual blue shift to 1764 cm⁻¹. The blue shift accompanied by the splitting of the one hydroxyl group band into two peaks at 3556 and 3570 cm⁻¹ is also well-rationalized by the existence of two types of -COOH groups in UPC-12 along with loss of the adsorbed CO₂ molecules according to the single-crystal analysis as detailed above. In addition, when the temperature is lowered in a gradual manner from 150 °C to room temperature for the sample also under a flowing N₂ atmosphere, no obvious change is observed in the in situ DRIFTS spectra (Figure S6), confirming again the strong adsorption of CO₂ gas to UPC-12 due to the intense hydrogen bonding and π - π interactions of

the CO₂ molecules with the uncoordinated carboxylate groups and bipy moieties, respectively, of UPC-12 at room temperature. At the end of this section, it is noteworthy that the present results reveal the great potential of both solid-state ¹³C CP-TOSS NMR spectroscopy and in situ DRIFTS in monitoring of CO₂ molecules adsorbed in porous MOF structures.

CONCLUSIONS

A porous Zn MOF (UPC-12) with exceptionally high thermal and chemical stability was synthesized in high yield and purity via a facile hydrothermal reaction based on low-cost commercially available starting materials. Gas adsorption measurements revealed the high selectivity of UPC-12 for CO₂ over N₂, CH₄, and H₂ due to hydrogen bonding and effective π ··· π interactions of the adsorbed CO₂ molecules with the -COOH groups located inside the channels of the framework and the π moieties (-C₆H₄N-) of the pillared bipy ligands of UPC-12, respectively, indicating the potential application of this MOF in selective capture/separation of CO₂ over N₂/CH₄/H₂. This was further supported by ¹³C NMR and in situ DRIFTS results and, more importantly, well-rationalized on the basis of DFT calculations. Further studies toward the design and synthesis of functional MOFs with high surface area and large channels decorated with more -COOH groups and therefore further improved selectivity for CO₂ gas are in progress.

ASSOCIATED CONTENT

Supporting Information

The Supporting Information is available free of charge on the ACS Publications website at DOI: 10.1021/acs.inorgchem.5b01232.

Details of gas adsorption experiments, calculation of isosteric heat of adsorption and adsorption selectivity, and additional figures (PDF)

Crystal structural data for UPC-12 (CIF)

The crystal structural data for UPC-12 have also been deposited with the Cambridge Crystallographic Data Centre (CCDC 1055675).

AUTHOR INFORMATION

Corresponding Authors

*E-mail: dfsun@upc.edu.cn.

*E-mail: jianzhuang@ustb.edu.cn.

Notes

The authors declare no competing financial interest.

ACKNOWLEDGMENTS

Financial support from the National Key Basic Research Program of China (Grants 2013CB933400 and 2012CB224801), the National Natural Science Foundation of China (Grants 21371179, 21271117, and 21290174), the Fundamental Research Funds for the Central Universities (13CX05010A), and NCET-11-0309 is gratefully acknowledged. We are also grateful to the calculating center of the Mining College of Guizhou University for the grant of computer time.

REFERENCES

- (1) (a) Stern, N. *Stern Review on the Economics of Climate Change*; Cambridge University Press: Cambridge, U.K., 2006; pp 233–250. (b) Jacobson, M. Z. *Energy Environ. Sci.* **2009**, *2*, 148–173.
- (2) Rochelle, G. T. *Science* **2009**, *325*, 1652–1654.
- (3) (a) Wilmer, C. E.; Farha, O. K.; Bae, Y.-S.; Hupp, J. T.; Snurr, R. Q. *Energy Environ. Sci.* **2012**, *5*, 9849–9856. (b) Morris, R. E.; Wheatley, P. S. *Angew. Chem., Int. Ed.* **2008**, *47*, 4966–4981.
- (4) Baker, R. W. *Ind. Eng. Chem. Res.* **2002**, *41*, 1393–1411.
- (5) (a) Li, J. R.; Sculley, J.; Zhou, H.-C. *Chem. Rev.* **2012**, *112*, 869–932. (b) Liu, J.; Thallapally, P. K.; McGrail, B. P.; Brown, D. R.; Liu, J. *Chem. Soc. Rev.* **2012**, *41*, 2308–2322. (c) Nugent, P.; Belmabkhout, Y.; Burd, S. D.; Cairns, A. J.; Luebke, R.; Forrest, K.; Pham, T.; Ma, S.-Q.; Space, B.; Wojtas, L.; Eddaoudi, M.; Zaworotko, M. J. *Nature* **2013**, *495*, 80–84.
- (6) (a) Nugent, P. S.; Rhodus, V. L.; Pham, T.; Forrest, K.; Wojtas, L.; Space, B.; Zaworotko, M. J. *J. Am. Chem. Soc.* **2013**, *135*, 10950–10953. (b) Bloch, W. M.; Babarao, R.; Hill, M. R.; Doonan, C. J.; Sumbly, C. J. *J. Am. Chem. Soc.* **2013**, *135*, 10441–10448.
- (7) D'Alessandro, D. M.; Smit, B.; Long, J. R. *Angew. Chem., Int. Ed.* **2010**, *49*, 6058–6082.
- (8) (a) Demessence, A.; D'Alessandro, D. M.; Foo, M. L.; Long, J. R. *J. Am. Chem. Soc.* **2009**, *131*, 8784–8786. (b) Zheng, B.-S.; Yang, Z.; Bai, J.-F.; Li, Y.-Z.; Li, S.-H. *Chem. Commun.* **2012**, *48*, 7025–7027. (c) Liao, P. Q.; Chen, H. Y.; Zhou, D. D.; Liu, S. Y.; He, C. T.; Rui, Z. B.; Ji, H. B.; Zhang, J. P.; Chen, X. M. *Energy Environ. Sci.* **2015**, *8*, 1011–1016.
- (9) (a) Vaidhyanathan, R.; Iremonger, S. S.; Shimizu, G. K. H.; Boyd, P. G.; Alavi, S.; Woo, T. K. *Science* **2010**, *330*, 650–653. (b) An, J.; Geib, S. J.; Rosi, N. L. *J. Am. Chem. Soc.* **2010**, *132*, 38–39. (c) Xue, D.-X.; Cairns, A. J.; Belmabkhout, Y.; Wojtas, L.; Liu, Y.; Alkordi, M. H.; Eddaoudi, M. *J. Am. Chem. Soc.* **2013**, *135*, 7660–7667. (d) Neofotistou, E.; Malliakas, C. D.; Trikalitis, P. N. *Chem. - Eur. J.* **2009**, *15*, 4523–4527.
- (10) (a) Lee, W. R.; Hwang, S. Y.; Ryu, D. W.; Lim, K. S.; Han, S. S.; Moon, D.; Choi, J.; Hong, C. S. *Energy Environ. Sci.* **2014**, *7*, 744–751. (b) Fracaroli, A. M.; Furukawa, H.; Suzuki, M.; Dodd, M.; Okajima, S.; Gandara, F.; Reimer, J. A.; Yaghi, O. M. *J. Am. Chem. Soc.* **2014**, *136*, 8863–8866. (c) Li, P. Z.; Zhao, Y. L. *Chem. - Asian J.* **2013**, *8*, 1680–1686.
- (11) (a) Wriedt, M.; Sculley, J. P.; Yakovenko, A. A.; Ma, Y. G.; Halder, G. J.; Balbuena, P. B.; Zhou, H. C. *Angew. Chem., Int. Ed.* **2012**, *51*, 9804–9808. (b) Britt, D.; Furukawa, H.; Wang, B.; Glover, T. G.; Yaghi, O. M. *Proc. Natl. Acad. Sci. U. S. A.* **2009**, *106*, 20637–20640. (c) Si, X. L.; Jiao, C. L.; Li, F.; Zhang, J.; Wang, S.; Liu, S.; Li, Z. B.; Sun, L. X.; Xu, F.; Gabelica, Z.; Schick, C. *Energy Environ. Sci.* **2011**, *4*, 4522–4527. (d) Li, P. Z.; Wang, X. J.; Zhang, K.; Nalaparaju, A.; Zou, R. Y.; Zou, R. Q.; Jiang, J. W.; Zhao, Y. L. *Chem. Commun.* **2014**, *50*, 4683–4685. (e) Wang, B.; Huang, H. L.; Lv, X. L.; Xie, Y. B.; Li, M.; Li, J. R. *Inorg. Chem.* **2014**, *53*, 9254–9259.
- (12) (a) Zheng, B. S.; Bai, J. F.; Duan, J. G.; Wojtas, L.; Zaworotko, M. J. *J. Am. Chem. Soc.* **2011**, *133*, 748–751. (b) Gassensmith, J. J.; Furukawa, H.; Smaldone, R. A.; Forgan, R. S.; Botros, Y. Y.; Yaghi, O. M.; Stoddart, J. F. *J. Am. Chem. Soc.* **2011**, *133*, 15312–15315. (c) Lin, J. B.; Zhang, J. P.; Chen, X. M. *J. Am. Chem. Soc.* **2010**, *132*, 6654–6656. (d) Lin, Q. P.; Wu, T.; Zheng, S. T.; Bu, X. H.; Feng, P. Y. *J. Am. Chem. Soc.* **2012**, *134*, 784–787.
- (13) (a) Comotti, A.; Gallazzi, M. C.; Simonutti, R.; Sozzani, P. *Chem. Mater.* **1998**, *10*, 3589–3596. (b) Comotti, A.; Bracco, S.; Sozzani, P.; Horike, S.; Matsuda, R.; Chen, J.; Takata, M.; Kubota, Y.; Kitagawa, S. *J. Am. Chem. Soc.* **2008**, *130*, 13664–13672. (c) Bassanetti, I.; Comotti, A.; Sozzani, P.; Bracco, S.; Calestani, G.; Mezzadri, F.; Marchio, L. *J. Am. Chem. Soc.* **2014**, *136*, 14883–14895. (d) Sozzani, P.; Bracco, S.; Comotti, A.; Ferretti, L.; Simonutti, R. *Angew. Chem., Int. Ed.* **2005**, *44*, 1816–1820. (e) Tian, J.; Ma, S. Q.; Thallapally, P. K.; Fowler, D.; McGrail, B. P.; Atwood, J. L. *Chem. Commun.* **2011**, *47*, 7626–7628.
- (14) (a) Delley, B. J. *J. Chem. Phys.* **1990**, *92*, 508. (b) Perdew, J. P.; Burke, K.; Ernzerhof, M. *Phys. Rev. Lett.* **1996**, *77*, 3865–3868.
- (c) Grimme, S. J. *J. Comput. Chem.* **2006**, *27*, 1787–1799. (d) McNellis, E. R.; Meyer, J.; Reuter, K. *Phys. Rev. B: Condens. Matter Mater. Phys.* **2009**, *80*, 205414.
- (15) Delley, B. J. *J. Chem. Phys.* **2000**, *113*, 7756–7764.
- (16) (a) Jiang, H. L.; Feng, D. W.; Wang, K. C.; Gu, Z. Y.; Wei, Z. W.; Chen, Y. P.; Zhou, H. C. *J. Am. Chem. Soc.* **2013**, *135*, 13934–13938. (b) Colombo, V.; Galli, S.; Choi, H. J.; Han, G. D.; Maspero, A.; Palmisano, G.; Masciocchi, N.; Long, J. R. *Chem. Sci.* **2011**, *2*, 1311–1319. (c) Kandiah, M.; Nilsen, M. H.; Usseglio, S.; Jakobsen, S.; Olsbye, U.; Tilset, M.; Larabi, C.; Quadrelli, E. A.; Bonino, F.; Lillerud, K. P. *Chem. Mater.* **2010**, *22*, 6632–6640.
- (17) Burd, S. D.; Ma, S. Q.; Perman, J. A.; Sikora, B. J.; Snurr, R. Q.; Thallapally, P. K.; Tian, J.; Wojtas, L.; Zaworotko, M. J. *J. Am. Chem. Soc.* **2012**, *134*, 3663–3666.
- (18) (a) Sozzani, P.; Bracco, S.; Comotti, A.; Ferretti, L.; Simonutti, R. *Angew. Chem., Int. Ed.* **2005**, *44*, 1816–1820. (b) Tian, J.; Ma, S. Q.; Thallapally, P. K.; Fowler, D.; McGrail, B. P.; Atwood, J. L. *Chem. Commun.* **2011**, *47*, 7626–7628.
- (19) Hu, Y.; Liu, Z. - X.; Xu, J.; Huang, Y. - N.; Song, Y. *J. Am. Chem. Soc.* **2013**, *135*, 9287–9290.